Electron-Electron Spin-Spin Interaction in Spin-Labeled Low-Spin Methemoglobin

Vladimir Budker, Jing-Long Du, Michael Seiter, Gareth R. Eaton, and Sandra S. Eaton
Department of Chemistry, University of Denver, Denver, Colorado 80208 USA

ABSTRACT Nitroxyl free radical electron spin relaxation times for spin-labeled low-spin methemoglobins were measured between 6 and 120 K by two-pulse electron spin echo spectroscopy and by saturation recovery electron paramagnetic resonance (EPR). Spin-lattice relaxation times for cyano-methemoglobin and imidazole-methemoglobin were measured between 8 and 25 K by saturation recovery and between 4.2 and 20 K by electron spin echo. At low temperature the iron electron spin relaxation rates are slow relative to the iron-nitroxyl electron-electron spin-spin splitting. As temperature is increased, the relaxation rates for the Fe(III) become comparable to and then greater than the spin-spin splitting, which collapses the splitting in the continuous wave EPR spectra and causes an increase and then a decrease in the nitroxyl electron spin echo decay rate. Throughout the temperature range examined, interaction with the Fe(III) increases the spin lattice relaxation rate ($1/T_1$) for the nitroxyl. The measured relaxation times for the Fe(III) were used to analyze the temperature-dependent changes in the spin echo decays and in the saturation recovery (T_1) data for the interacting nitroxyl and to determine the interspin distance, r. The values of r for three spin-labeled methemoglobins were between 15 and 15.5 Å, with good agreement between values obtained by electron spin echo and saturation recovery. Analysis of the nitroxyl spin echo and saturation recovery data also provides values of the iron relaxation rates at temperatures where the iron relaxation rates are too fast to measure directly by saturation recovery or electron spin echo spectroscopy. These results demonstrate the power of using time-domain EPR measurements to probe the distance between a slowly relaxing spin and a relatively rapidly relaxing metal in a protein.

INTRODUCTION

The first published suggestion that interaction of paramagnetic metals with nitroxyl spin labels might affect the spin label EPR spectrum was a question by Symons after a presentation by McConnell (McConnell and Boeyens, 1967). No effect was observed (McConnell and Boeyens, 1967; McConnell and Hamilton, 1968), but it was predicted that "there is a reasonable chance that a spin-spin interaction could be detected at low temperatures in methemoglobin" (McConnell and Boeyens, 1967). This predicted effect has been observed (Asakura and Drott, 1971; Asakura and Lau, 1978), but with one exception has not been quantitatively characterized for hemoglobin spin labeled at the β-93 cysteine, the position most commonly labeled. The spin label continuous wave (CW) EPR changes upon deoxygenation of β93-spin-labeled hemoglobin were interpreted with the Leigh (1970) model as showing a distance of 12.5 Å between the label and the iron (Asakura and Lau, 1978). However, there has been a quarter century of spin label studies of hemoglobin and myoglobin from various mammals, emphasizing oxygen binding, conformational changes, etc., in which iron-nitroxyl magnetic interaction was not part of the interpretation (McConnell and Boeyens, 1967; McConnell et al., 1969; Ho et al., 1970; McConnell, 1971; Ogata and McConnell, 1971; Chien et al., 1980; Steinhoff, 1990). It has been noted, for example, that changing the spin state of the iron in spin-labeled horse hemoglobin affects the CW EPR spectrum of the nitroxyl spin label in a way that was interpreted as reflecting protein structural changes (McConnell et al., 1969). In related experiments, iron-nitroxyl interaction was observed in a hemoglobin reconstituted with a heme spin labeled at the propionic acid side chain (Asakura et al., 1972).

X-ray crystallography of spin-labeled horse carboxyhemoglobin, consistent with earlier EPR results, found two conformational states of the spin label relative to the protein when β93-cys was labeled with iodoacetamide spin label (Moffat, 1971). In one conformation the spin label points into the protein and displaces tyrosine β145, and in the other conformation it points out from the protein. These conformations correspond, respectively, to the more immobilized and less immobilized labels observed in EPR studies (McConnell and Hamilton, 1968; McConnell et al., 1969). The conformation of the spin label depends on the iron ligation, pH, and other environmental conditions. EPR crystallography (oriented single crystal EPR) has revealed the orientations of two types of spin label and heme in spin-labeled horse oxyhemoglobin (diamagnetic iron), methemoglobin fluoride (high spin) and methemoglobin azide (low spin) (Chien, 1979). More than one spin label orientation relative to the crystal axes was found in some cases. No spin-spin interaction was observed and no distance information was obtained. Orientation dependence of CW EPR parameters has been measured for single crystals of metmyoglobin (Scholes et al., 1982).

Interaction between β93 spin label and Cu(II) at various binding sites or replacing iron in hemoglobin has been interpreted in terms of the Leigh (1970) model (Antholine et al., 1985; Manoharan et al., 1990). As discussed below,

Received for publication 6 February 1995 and in final form 23 March 1995.
Address reprint requests to Dr. Sandra Eaton, Department of Chemistry, University of Denver, Denver, CO 80208. Tel.: 303-871-3102; Fax: 303-871-2254; E-mail: seaton@cair.du.edu.

0006-3495/95/06/2531/12 $2.00

information about relaxation times requires reanalysis of these results. The current question of whether there is a relation between quaternary structure and metal spin state (Marden et al., 1991; Kelleher, 1993) requires sensitive and accurate measures of distances within metalloproteins.

Prior attempts to estimate the interaction between spin labels and the iron in hemoglobin or myoglobin have relied upon changes in the shape and apparent intensity of the CW EPR spectrum. To the extent that the nitroxyl EPR lineshape is determined by interaction with a paramagnetic iron, a large change in relaxation time is required to cause a significant increase in linewidth beyond that caused by unresolved hyperfine splitting and by g- and a-anisotropy. The direct measurement of nitroxyl electron spin lattice relaxation time (T_1) and electron spin phase memory relaxation time (T_m) is potentially both a more sensitive and more accurate measure of distance and of the paramagnetism of the metal. In this paper we apply to nitroxyl spin-labeled low-spin hemoglobin the time-domain EPR techniques for measuring interspin distances recently developed and calibrated with model compounds (Rakowsky et al., 1995). While there remain many detailed questions about the reaction chemistry and structural chemistry of hemoglobin, there is also a large enough body of information to put sufficiently reasonable limits on derived results that hemoglobin is the choice for application of our recently proposed modified Bloembergen equations and analysis of electron spin echoes (ESEs), which includes direct measurements of the relaxation times for the fast relaxing metal (Rakowsky et al., 1995).

MATERIALS AND METHODS

Preparation of spin-labeled hemoglobins

Oxy-hemoglobin (oxy-Hb) was isolated from freshly drawn human blood following the procedure of Caughey et al. (1985) (V. Sampath, M. R. Gunther, and W. S. Caughey, submitted for publication). Immediately upon completion of the isolation procedure the protein (5–6 mM in heme) was frozen with liquid nitrogen in 0.3–1.0-ml aliquots in plastic microfuge tubes and stored at −60°C. In the following paragraphs values of ϵ are given in M^{-1} cm^{-1} where molarity is the heme concentration.

Spin labeling with 4-(2-iodoacetamido)-TEMPO (Sigma Chemical Co., St. Louis, MO) to prepare oxy-Hb-ISL or with 4-maleimido-TEMPO (Sigma Chemical Co.) to prepare oxy-Hb-MSL followed the procedure of Manoharan et al. (1990). The concentration of the oxyhemoglobin was determined from the absorbance of the Soret band (415 nm, $\epsilon = 1.25 \times 10^5$ M^{-1} cm^{-1}) (Antonini and Brunori, 1971). The concentration of spin label in oxy-Hb-ISL or oxy-Hb-MSL was determined by double integration of the room temperature CW EPR spectrum of the nitroxyl signal and comparison with the double integral of a spectrum for a known concentration of 2,2,6,6-tetramethylpiperidin-1-oxyl (TEMPO). The comparisons showed 0.45–0.5 spin labels per hemoglobin monomer, which corresponds to 90–100% labeling of the β subunits. Unreacted sulfhydryl groups were assayed with 2,2′-dithiopyridine (Brocklehurst and Little, 1973; Grassetti and Murray, 1967).

MetHb, metHb-ISL and metHb-MSL were prepared from oxy-Hb, oxy-Hb-ISL or oxy-Hb-MSL, respectively, by treatment with $K_3Fe(CN)_6$ (DiIorio, 1981). Conversion to the met form was monitored by the absorbance at 500 nm ($\epsilon = 1.0 \times 10^4$ M^{-1} cm^{-1}) (Scheler et al., 1957). CN-metHb, CN-metHb-ISL and CN-metHb-MSL were prepared by addition of KCN solution to produce a 2:1 ratio of CN^- to met-heme. Im-metHb and Im-metHb-ISL were prepared by addition of a 1 M solution of imidazole in water at pH 8 to the methemoglobin sample in 10 mM potassium phosphate buffer at pH 6.8, with a final imidazole concentration of 100 mM. Coordination was monitored by following the absorbance at 534 nm ($\epsilon = 1.47 \times 10^4$ M^{-1} cm^{-1}) (DiIorio, 1981). K_d is ~16 mM.

Samples for EPR spectroscopy were prepared in 10 mM phosphate buffer, pH 6.8, diluted 1:1 with glycerol, with a final concentration of spin label between 0.5 and 1.0 mM. In the presence of glycerol and CN^- the spin labels rapidly undergo a redox reaction that destroys the paramagnetic center, so these samples were frozen immediately after preparation. Although other samples appear to be stable, samples were prepared shortly before the EPR spectroscopy and stored in liquid nitrogen. With the exception of the oxyhemoglobin samples, solutions were degassed by several freeze-pump-thaw cycles. Samples for liquid helium measurements in the Oxford ESR900 cryostat were back-filled with 1–2 torr of nitrogen or helium to improve heat transfer and sealed. Sample tubes for measurements on the ESP380E with the Oxford 935 cryostat were back-filled with helium, and the open tubes were placed in the cryostat to facilitate thermal equilibration with the cold helium atmosphere.

CW EPR spectra

CW EPR spectra at room temperature or liquid nitrogen temperatures were obtained on a Bruker ER200 with a TE_{102} rectangular resonator and 100 kHz magnetic field modulation. Microslides (0.4 mm path length) (Eaton and Eaton, 1977) or 1.0 mm melting point capillaries were used for room temperature spectra. Quartz tubes (4.0 mm outside diameter (OD)) were used for liquid nitrogen and liquid helium spectroscopy. Spectra at liquid helium temperatures were obtained on a Bruker ESP380E spectrometer operating at 9.71 GHz with a dielectric resonator and an Oxford CF935 cryostat. CW spectra of the nitroxyl portions of the spectra at 8 to 50 K were recorded with 1.56 kHz magnetic field modulation and 2.6×10^{-4} mW microwave power to minimize power saturation and passage effects. The spectra at 8 K were recorded with both increasing and decreasing magnetic field to check for passage effects. CW spectra of the iron signals were obtained with 100 kHz magnetic field modulation and microwave powers that did not cause power saturation.

Saturation recovery (SR) measurements

A locally constructed spectrometer (Quine et al., 1992) was used for the SR measurements. Temperatures between 5 and 70 K were obtained with liquid helium and an Oxford ESR900 flow cryostat. Temperatures between 80 and 120 K were obtained with liquid nitrogen and a Varian dewar flow assembly. To test for spectral diffusion the pump time was increased until further increase gave no detectable change in the recovery time constant. Pump times used for data collection were $>T_1$. Typically 5000–10,000 recovery curves were signal averaged in a LeCroy digital oscilloscope and transferred to a PC for data analysis. Data were fit to a single exponential with locally written software.

ESE measurements

ESE decays were recorded on a locally constructed spectrometer operating at ~9.2 GHz with an over-coupled Varian V4531 TE_{102} resonator (Quine et al., 1987) or on a Bruker ESP380E with a dielectric resonator operating at 9.71 GHz. A 90-τ-180-τ-echo sequence was used. The time for a 90° pulse was 20 ns on the locally constructed spectrometer and ~13 ns on the ESP380E. Echo decays of 256, 512, or 1024 data points were recorded starting at 80–120 ns and extending for 2–15 μs. On the locally constructed spectrometer the boxcar aperture was set to encompass the full width of the echo. On the ESP380E an integrator was used to digitize the full echo. On the locally constructed system temperatures between 5 and 70 K were obtained with an Oxford ESR900 flow cryostat. For both the SR and ESE systems, temperatures in the ESR900 were calibrated by replacing the sample-containing tube with a tube containing a thermocouple immersed in 1:1 water:glycerol. On the ESP380E an Oxford 935 cryostat was used to

obtain temperatures between 4 and 70 K. Sample temperatures were calibrated with a Lakeshore 820 readout and a TG-120PL GaAlAs diode immersed in silicone oil in a 4 mm OD quartz EPR tube that replaced the sample tube. The diode and readout had been calibrated recently. The uncertainty in temperature is estimated to be ±1 K.

The time constant for the ESE decay is referred to as T_m to encompass all processes that result in echo dephasing (see discussion below). The values obtained directly from experiment are typically cited as decay time constants. In the ensuing discussion it is often more direct to refer to relaxation rates, which are the reciprocals of the time constants.

For 1 mM frozen solutions at the temperatures and pulse lengths examined in these studies, nitroxyl T_m is weakly dependent upon B (the microwave magnetic field), which indicates that instantaneous diffusion (Salikhov and Tsvetkov, 1979) due to spin flips of a neighboring radical during the second microwave pulse makes a minor contribution to T_m. To the extent that this process contributes to T_m it will be about the same for spin label in the presence of diamagnetic or paramagnetic heme and does not contribute to differences between oxy-Hb-SL and low-spin metHb-SL. (The low-spin Fe(III) EPR signal extends over ~2000 G so the probability that a neighboring Fe(III) is flipped by the second microwave pulse and thereby changes the resonance of the interacting nitroxyl is negligibly small.) For Im-metHb and CN-metHb the value of T_m was independent of microwave B_1, which indicates that instantaneous diffusion makes a negligible contribution to the dephasing process (Salikhov and Tsvetkov, 1979). For the iron signals there was no indication of dynamic processes contributing to T_m, so T_m is a reasonable estimate of the low-spin Fe(III) T_2.

ANALYSIS OF EXPERIMENTAL DATA

Analysis of CW spectra

CW spectra of Oxy-Hb-ISL at 100 K, CN-metHb and Im-MetHb at 10 K were analyzed with the locally written program MONMER, which uses perturbation calculations, assumes that the principal axes of the **g** and **A** matrices are co-linear, and treats hyperfine interactions to second order (Toy et al., 1971). The derived nitroxyl parameters are: g_x= 2.0095, g_y=2.0053, g_z = 2.0025, $A_x = 4 \times 10^{-4}$, $A_y = 7 \times 10^{-4}$, $A_z = 35 \times 10^{-4}$ cm^{-1}. The relative values of the g components are more precise than the absolute values because of uncertainties in the external field calibration. The parameters for low-spin Fe(III) in CN-metHb are g_x = 1.45, g_y = 1.65, and g_z = 3.52, and for Im-metHb are 1.44, 2.22, and 3.02.

Estimates of the approximate range of interspin distances consistent with the overall distortion of the CW spectra of the spin-labeled methemoglobins at low temperature were obtained by simulations with the locally written program, MENO (Eaton et al., 1983). This perturbation calculation includes the effects of anisotropic g values and arbitrary relative orientations of the **g** matrices for the two centers.

The x-ray crystal structure of spin-labeled hemoglobin was reported (Moffat, 1971), but does not appear to be available in electronically readable format. The x-ray crystal structure of oxy-Hb (Shaanan, 1983) was downloaded from the Brookhaven Protein Data Base (Berstain et al., 1977) and read into HyperChem (Hyper Cube, Inc., Toronto, Canada). One β subunit was selected for examination. The β-93 cys was mutated to a spin label analog in which the N—O is replaced by a carbonyl group (Hartmann et al., 1991). Without energy optimization the distance between the heme iron and the midpoint of "spin label" CO (pseudo-NO) bond was 14.8 Å. Two attempts at energy optimization starting from different rotamers of the "spin label" side chain and without water of hydration resulted in heme iron to "NO" distances of 16.9 and 17.4 Å. These calculations are not likely to represent exact structures, but were performed to obtain estimates of heme iron to nitroxyl distances and suggest that plausible distances are in the range of 14.5–17.5 Å.

Analysis of SR data for spin-labeled complexes

The relaxation of one type of spin by another type of spin was described by Bloembergen et al. (1948, 1949, 1959), in an NMR context and can be expressed as in Eq. 1 (Kulikov and Likhtenshtein, 1977).

$$\frac{1}{T_{1s}} = \frac{1}{T_{1s}^{o}} + S(S+1) \times \left[\underbrace{\frac{b^2 T_{2f}}{1 + (\omega_f - \omega_s)^2 T_{2f}^2}}_{\text{(B term)}} + \underbrace{\frac{c^2 T_{1f}}{1 + \omega_s^2 T_{1f}^2}}_{\text{(C term)}} + \underbrace{\frac{e^2 T_{2f}}{1 + (\omega_f + \omega_s)^2 T_{2f}^2}}_{\text{(E term)}} \right] \quad (1)$$

$$b^2 = \frac{8}{3}\left[-\frac{J}{2} - \frac{1}{4} g_s g_f \beta^2 \frac{(1 - 3\cos^2\theta)}{\hbar r^3} \right]^2$$

$$c^2 = 3 g_s^2 g_f^2 \beta^4 \frac{\sin^2\theta \cos^2\theta}{\hbar^2 r^6}$$

$$e^2 = 3 g_s^2 g_f^2 \beta^4 \frac{\sin^4\theta}{\hbar^2 r^6}$$

where "f" and "s" denote the fast and slow relaxing spins, respectively, T_{1s}^{o} is T_1 for the slowly relaxing spin in the absence of spin-spin interaction, T_{1s} is T_1 for the slowly relaxing spin perturbed by the fast relaxing spin, S is the electron spin on the faster relaxing center, ω_f and ω_s are the resonant frequencies for the fast and slow relaxing spins, respectively, r is the interspin distance, J is the electron-electron exchange interaction for the Hamiltonian written as $-JS_1 \cdot S_2$, and θ is the angle between the interspin vector and the external magnetic field.

Two modifications of this equation were introduced to adapt it for use in the computer program MENOSR to analyze frozen solution SR data. 1) $\omega_f - \omega_s$ ($\Delta\omega$) is calculated from the anisotropic g values of the unpaired electrons for each orientation of the molecule with respect to the external field. 2) Eq. 1 was originally derived for NMR cases where $\Delta\omega$ is large relative to the spin-spin interaction, which is the first-order or AX approximation. In EPR spectra with overlapping signals, $\Delta\omega$ may be quite small. In the limit where $\Delta\omega$ is small enough that the denominator of the B term goes to 1, Eq. 1 predicts that the effect on $1/T_{1s}$ is proportional to T_{2f}, which is not reasonable. To exactly describe the contribution to $1/T_{1s}$ as $\Delta\omega$ decreases would require equations comparable to those used in calculations of AB splitting patterns (Eaton et al., 1983). Based on data obtained for the effect of Cu(II) on T_1 of nitroxyl radicals (Rakowsky et al., 1995) we propose that a reasonable approximation can be

obtained by replacing the B term in Eq. 1 with Eq. 2.

$$\text{B term} = \frac{b^2 T_{2f}}{1 + (\omega_f - \omega_s)^2 T_{2f}^2 + b^2 T_{1f} T_{2f}}. \quad (2)$$

The additional term in the denominator of Eq. 2 is negligible when $\Delta\omega T_{2f}$ is large; however, it ensures that in the limit of small $\Delta\omega$ and/or strong interaction (large b), the limiting contribution to $1/T_{1s}$ is $1/T_{1f}$. The physical model is as follows. For cases of relatively weak spin-spin interaction as examined in this paper, the interaction can only enhance the spin lattice relaxation rate of the slower relaxing center to the extent that it becomes equal to the spin lattice relaxation rate of the faster relaxing center. This limiting behavior can also be important when the metal T_2 is significantly shorter than the metal T_1.

A random distribution of molecular orientations with respect to the external magnetic field was included in the computer simulations using MENOSR. For each of those molecules there is a defined orientation of the interspin vector relative to the axes of the iron **g** matrix. Orientation selection was not included in the calculations. In the spin-labeled methemoglobins the nitroxyl T_1 showed little variation with position in the EPR spectrum. At X-band, possibilities for orientation selection based on position in the nitroxyl CW spectrum are limited by the orientation dependence of the nitroxyl nitrogen hyperfine splitting (~30 G). The selectivity is decreased by unresolved proton hyperfine coupling, which contributes ~7 G to the linewidths in frozen solution. The interspin distances used in the calculations (~15 Å) result in maximum dipolar splittings that are of the same order of magnitude as the nitroxyl hyperfine splitting, which largely eliminates possibilities for orientation selection at these interspin distances.

Analysis of spin echo data

Bloembergen's work also predicts an effect of the fast relaxing spin on T_2 for the slower relaxing spin (Bloembergen et al., 1948, 1959; Bloembergen, 1949; Kulikov and Likhtenshtein, 1977). Most of the terms in the expression given by Kulikov and Likhtenshtein (1977) for the impact on T_2 are spectral density functions analogous to those in the expression for the impact on T_1 (Eq. 1). Between 4 and 150 K nitroxyl T_m values are orders of magnitude shorter than T_1. Thus, terms that are significant with respect to $1/T_1$ for nitroxyl are negligible with respect to $1/T_m$. However, in the expression for the impact of the fast relaxing spin on T_2 of the slowly relaxing spin there is an additional term, Eq. 3 (Kulikov and Likhtenshtein, 1977).

$$\frac{\mu^2\gamma^2 T_{1f}}{3r^6}(1 - 3\cos^2\theta)^2 \quad (3)$$

where μ is the magnetic moment of the fast relaxing spin, γ is the electron magnetogyric ratio, T_{1f} is T_1 for the fast relaxing spin, θ is the angle between the magnetic field and the interspin vector, and r is the interspin distance.

This term reflects the effect on nitroxyl T_2 due to dynamic collapse of the dipolar splitting in the limit where the metal relaxation rate is fast relative to the magnitude of the splitting, i.e., the fast exchange limit (Nakagawa et al., 1992). This term is the dominant effect of the Fe(III) on the nitroxyl ESE data in the temperature regime examined by this report. It can be treated for the full range of metal relaxation rates relative to the spin-spin splittings (both exchange and dipolar) as described in the following paragraph.

Zhidomirov and Salikhov (1969) presented the following expression for the impact on the ESE curve of a process that they called "spectral diffusion" in a spin-coupled system.

$$E(2\tau) = R^{-2}\{\exp(-2\tau/\tau_C)[\tau_C^{-2}\sinh^2(R\tau) + R^2\cosh^2(R\tau) + R\tau_C^{-1}\sinh(2R\tau) + \Delta^2\sinh^2(R\tau)]\} \quad (4)$$

where $E(2\tau)$ is the intensity of the echo as a function of τ; τ is the time between microwave pulses in the two-pulse experiment; τ_C is the correlation time for the dynamic process; Δ is ½ the angular frequency difference between the two sites averaged by the dynamic process; and $R^2 = \tau_C^{-2} - \Delta^2$.

The original expressions (Zhidomirov and Salikhov, 1969) used T_{1f} as τ_C. It was subsequently recognized that this expression could be used to analyze the effects on spin echo decay due to rotation of a methyl group coupled to an unpaired electron (Kispert et al., 1982). In this case τ_C is the correlation time for the rotation process.

When τ_C is significantly larger or smaller than $|\Delta|$, Eq. 4 can be simplified (Kispert et al., 1982). The expressions for the rate constants in these simplified forms are the same as those that are used to obtain approximate rate constants from linewidths in dynamic NMR experiments (Nakagawa et al., 1992), which makes it clear that the same fundamental principles underlie the interpretation of dynamic NMR lineshapes, the collapse of the spin-spin splittings in CW EPR spectra and the impact of electron spin relaxation of the fast-relaxing spin on the ESE data for the slowly relaxing spin in a spin-coupled system. The limiting forms of Eq. 4 (Kispert et al., 1982) and the regimes in which they were used to improve numerical stability in the program TMDYNAM are given in Eqs. 5 and 6.

for the slow averaging limit $(1/\tau_C < 0.08|\Delta|)$

$$E(2\tau) = \exp(-2\tau/\tau_C) \quad (5)$$

for the fast averaging limit $(1/\tau_C > 5|\Delta|)$

$$E(2\tau) = \exp\left[-2\tau\left(\frac{\Delta^2\tau_C}{2}\right)\right] \quad (6)$$

Zhidomirov and Salikhov (1969) proposed the use of T_{1f} as τ_C for the spin-coupled pair. In analyzing the spin echo data in this study it was found that $\tau_c = \sqrt{(T_{1f}T_{2f})}$ gives better agreement with the experimental data than $\tau_c = T_{1f}$. In analyzing a different problem Wolf (1966) has shown that for inhomogeneously broadened lines, the statistics can give τ_c

$= \sqrt{(T_{1f}T_{2f})}$. For the spin-coupled pair Δ is the orientation-dependent spin-spin splitting, which includes the dipole and exchange contributions. In TMDYNAM Δ is calculated from the expressions that have been used to analyze the spin-spin splitting in CW EPR spectra (Eaton et al., 1983). The value of Δ was calculated for each orientation of the molecule in the magnetic field. Depending upon the relative values of $1/\tau_C$ and Δ, Eq. 4, 5,or 6 was used to calculate the echo decay curve for that orientation. The calculated echo decay curve was multiplied by a single exponential with decay constant T_m to account for other nitroxyl relaxation processes. The powder average decay curve for the frozen solution samples was obtained by summing the contributions from a spherical average of orientations.

The impact of orientation selection was tested in the calculations. Only those orientations of the molecule having resonance fields within a specified window around the observing fields were included in the calculated summation. Most of the experimental ESE data were recorded at a magnetic field in the center of the nitroxyl spectrum with a microwave B_1 of ~5 Gauss. In addition, the unresolved proton hyperfine splitting spreads the signal from a particular orientation of the molecule over ~7 G (the inhomogeneously broadened linewidth required to simulate the CW spectra at 100 K). Because of the magnitude of B_1, the proton hyperfine interaction, and the overlapping contributions from g_x, g_y, and g_z, decay curves calculated with orientation selection at the center of the spectrum (a window of 5–7 Gauss) agreed within experimental noise levels with curves calculated without orientation selection. At a few temperatures ESE data were recorded as a function of position in the spectrum and indicated some orientation selection at the extremes of the spectra.

Selection of parameters

The parameters needed in Eqs. 1, 2, and 4–6 are: r, the distance between the low-spin Fe(III) and the nitroxyl; J, the electron-electron exchange coupling constant; the g values for the two paramagnetic centers; the orientation of the interspin vector relative to the g axes of the low-spin iron; the T_1 and T_2 values for the low-spin iron; and T_1 and T_m for nitroxyl in the absence of the interaction with the Fe(III). Several of these parameters were obtained directly from samples containing only one of the paramagnetic centers. The iron and nitroxyl g values were calculated by simulation of spectra for CN-metHb, Im-MetHb and oxyHb-ISL. Nitroxyl T_1 and T_m in the absence of spin-spin interaction were obtained by SR and ESE measurements of oxyHb-ISL. In the absence of interaction with Fe(III) the nitroxyl T_1 is dependent upon position in the spectrum (Du et al., 1995). The values of T_1 at the magnetic field at which the SR data were obtained for the spin-coupled complex were used in the calculations with MENOSR. In the absence of interaction with Fe(III) the nitroxyl T_m is independent of position in the spectrum at the temperatures for which the impact of Fe(III) was examined (4–60 K), which indicates that motional effects that cause orientation-dependent variation of T_m for metal complexes (Du et al., 1992) are not significant for nitroxyl radicals in water:glycerol in this temperature regime. T_1 and T_2 for low-spin Fe(III) in CN-metHb and Im-metHb were obtained directly by SR (between 6 and 20) or ESE (between 4.2 and 20 K). T_m for the Fe(III) signals showed no variation with position in the spectrum, within experimental uncertainty. At 8 K T_1 for CN-Hb decreased monotonically with increasing field between 2000 and 5000 G, with a total spread of ~40%. Because this variation is small relative to the temperature dependence, it was not included in the calculations. The temperature dependence of T_1 for the low-spin Fe(III) centers was measured at 3000 G. The distance between nitroxyl on one β chain and the iron of an adjacent α chain is ~35 Å, which is so much longer than the iron-nitroxyl distance within a chain that these additional interactions were neglected.

The definitions of the angles that relate orientations of the interspin vector and the **g** matrices for the two paramagnetic centers are the same as used in MENO (Fig. 1 in Eaton et al., 1983). The angle between the interspin vector and the z axis of the **g** matrix of spin 1 is ϵ and the angle between the

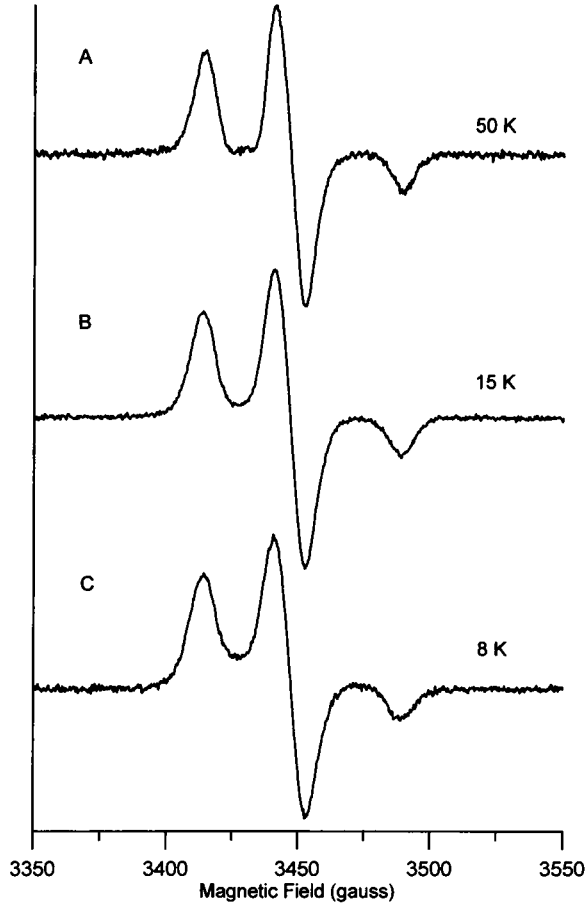

FIGURE 1 CW EPR spectra of Im-metHb-ISL as a function of temperature at 9.68 GHz obtained with 1.56 kHz magnetic field modulation and 2.6 $\times 10^{-4}$ mW microwave power. (*A*) 50 K, 0.10 G modulation amplitude, 168 s sweep time; (*B*) 15 K, 0.051 G modulation amplitude, 168 s sweep time; (*C*) 8 K, 0.010 G modulation amplitude, 670 s sweep time.

projection of the interspin vector and y axis of the **g** matrix for spin 1 is η (Eaton et al., 1983). In the orientation-selected calculations of the spin echo data the nitroxyl was defined as spin 1 and the Fe(III) as spin 2. In orientation-selected calculations of the ESE decays the angle between the z axis of the nitroxyl **g** matrix and the z axis of the Fe(III) **g** matrix is denoted A_1 and the angle between the projection of the nitroxyl z axis on the xy plane of the Fe(III) axes and the Fe(III) x axis is denoted A_2 (Eaton et al., 1983). The calculated echo decay curves for magnetic fields in the center of the spectrum, with the 5–7 Gauss orientation selection window or without orientation selection, were weakly dependent upon the relative orientations of the iron and nitroxyl **g** matrices. In the calculations of the spin echo decays for CN-metHb-MSL shown below the angles are $\epsilon = 20°$, $\eta = 30°$, $A_1 = 25°$, and $A_2 = 45°$. In the calculations of the SR curves the Fe(III) is spin 1 and nitroxyl is spin 2. The calculated SR curves shown below were obtained for $\epsilon = 25°$, $\eta = 45°$. The calculated SR curves were weakly dependent upon these relative orientation parameters. It was not possible to test all combinations of ϵ, η, A_1, and A_2, but checks on random combinations indicated that values of r that give acceptable match with the experimental data for different combinations of the angles differed by <1 Å.

The shortest through-bond pathway between the heme and the nitroxyl moiety attached at the β-93 sulfhydryl is 17 bonds, so a strong electron-electron exchange interaction is unlikely. The lineshapes of the nitroxyl signals in the CW spectra also rule out the possibility of a strong exchange interaction. In the low-spin Fe(III) complexes the unpaired electron is in d_{xz}, which provides a relatively inefficient pathway for spin delocalization into the heme ring or to axial ligands, suggesting weak exchange interaction. SR and ESE data were analyzed first assuming $J = 0$. Addition of non-0 values of J were then tested to determine whether fit to the data was improved. If J dominates the spin-spin interaction, Δ (in Eqs. 4–6) is approximately isotropic and the echo decay approaches a single exponential. If dipolar interaction dominates, Δ is highly anisotropic and the echo decay consists of a distribution of exponential decays. In the SR data for the low spin Fe(III) complexes examined here, the B term in Eqs. 1 and 2 dominates. A distribution of SR decay constants is observed even when J dominates the spin-spin interaction because of the anisotropy in $\Delta\omega$. However, the width of the distribution is increased by increasing dipolar contributions.

RESULTS

As demonstrated by McConnell and Hamilton (1968), hemoglobin can be selectively spin labeled at the β-93 cysteine. When iodo-acetamido or maleimido spin labels were reacted with oxy-Hb, quantitation of the EPR spectra of the oxy-Hb-ISL or oxy-Hb-MSL confirmed the addition of two labels per tetramer, consistent with specific labeling at β-93 cysteine. Tests with 2,2′-dithiopyridine (Brocklehurst and Little, 1973; Grassetti and Murray, 1967) confirmed that reactive sulfhydryl groups that were present before attachment of the spin label are not available after labeling.

CW spectra

The CW spectra of the nitroxyl signals for Im-metHb-ISL and CN-metHb-MSL between 8 and 50 K are shown in Figs. 1 and 2. At 50 K the spectra are typical of immobilized nitroxyl radicals and show no evidence of distortion due to electron-electron spin-spin interaction. As the temperature is decreased, there is increasing distortion of the spectra, although resolved splittings are not observed. At 8 K identical spectra were obtained for upfield and downfield scans, which indicates that the distortions in the lineshape were not due to passage effects. Severe passage effects due to the long nitroxyl T_1 prevented collection of valid CW spectra at temperatures lower than ~8 K. The temperature dependence of the spectra is due to changes in the relaxation rate of the Fe(III). At low temperature the iron relaxation rates (in Hz) are slow relative to the electron-electron spin-spin splitting (in Hz) and the nitroxyl spectra are distorted by the unresolved splittings (Eaton and Eaton, 1988a, 1989). As the

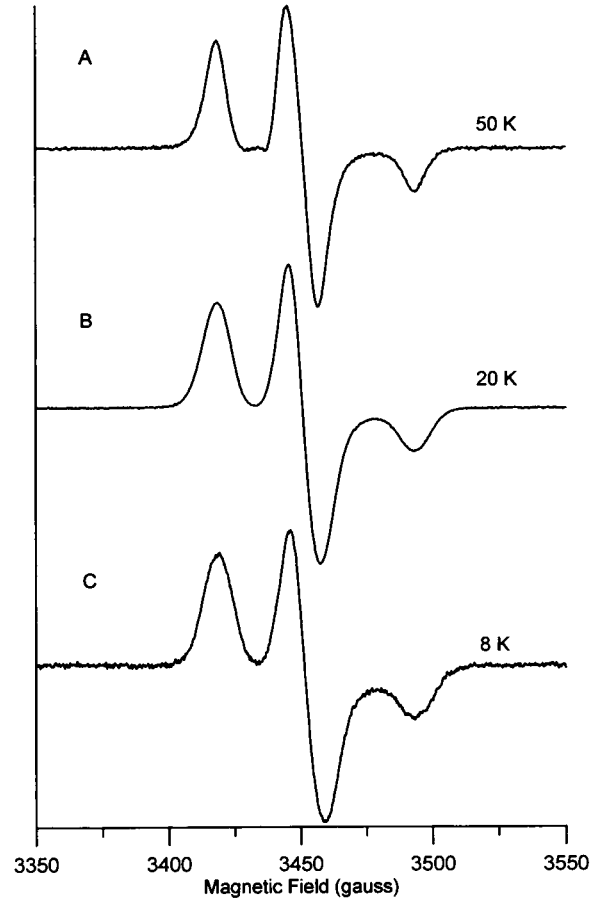

FIGURE 2 CW EPR spectra of CN-metHb-MSL as a function of temperature at 9.70 GHz obtained with 1.56 kHz magnetic field modulation and 2.6×10^{-4} mW microwave power. (*A*) 50 K, 0.10 G modulation amplitude, 168 s sweep time; (*B*) 20 K, 0.10 G modulation amplitude, 168 s sweep time; (*C*) 8 K, 0.012 G modulation amplitude, 168 s sweep time.

temperature is increased, the iron relaxation rates become sufficiently fast for the spin-spin splittings to be collapsed. This temperature dependence is an EPR analog of dynamic NMR (Drago, 1992) in which the temperature-dependent process is the iron relaxation. Although the lack of resolved features due to spin-spin splitting in the low temperature spectra prevent a unique simulation of the CW spectra, simulations can provide estimates of plausible values of r. These values are summarized in Table 1.

ESEs

In an ESE experiment the echo intensity is recorded as a function of the time between the two echo-forming microwave pulses. The time constant for the decay is commonly called the phase memory time, T_m, and includes contributions from all processes that lead to loss of phase coherence of the electron spins. These processes include motion of the molecule as a whole that changes the resonance frequency of a spin (Du et al., 1992), exchange processes such as methyl rotation (Nakagawa et al., 1992; Dzuba et al., 1981; Tsvetkov and Dzuba, 1990; Du et al., 1994), spin-spin relaxation between the observed spin and matrix electron and/or nuclear spins (T_2), and in the case of interest here the spin relaxation of an electron to which the observed electron is spin coupled.

Below ~60 K, $1/T_m$ for oxy-Hb-ISL is approximately independent of temperature (Fig. 3), which is typical of the behavior of nitroxyl radicals (Nakagawa et al., 1992). The limiting relaxation rate at low temperature is due to matrix nuclei. Above ~60 K the nitroxyl T_m decreases because of rotation of the methyl groups at rates comparable to the magnitude of the electron-proton couplings (Nakagawa et al., 1992; Dzuba et al., 1981; Tsvetkov and Dzuba, 1990). For the spin-labeled low-spin hemoglobins $1/T_m$ is strongly temperature dependent (Fig. 3 and 4). As the temperature is increased from 8 to ~20 K (Figs. 3 and 4, *curves A, B,* and *C*) the echo decay rate increases dramatically. As the temperature is increased further, the decay rate decreases (Figs. 3 and 4, *curves D* and *E*). The temperature dependence of $1/T_m$ observed for these complexes is typical of systems undergoing a dynamic process (Nakagawa et al., 1992; Dzuba et al., 1981; Tsvetkov and Dzuba, 1990). These changes in T_m occur in the same temperature interval in which the CW lineshapes were temperature dependent (Figs. 1 and 2). The dynamic process that impacts the ESE decay times is therefore assigned to the same process that affects the lineshapes, i.e., the collapse of the iron-nitroxyl spin-spin interaction due to increasing rates of iron electron spin relaxation.

To quantitatively interpret the changes in nitroxyl T_m due to interaction with the Fe(III), values are needed for the Fe(III) relaxation rates. SR and ESE spectroscopy were used to measure T_1 and T_2, respectively, for the low-spin Fe(III) in CN-metHb and Im-metHb between 6 and 25 K. These data are shown as solid symbols in Figs. 5 and 6. The solid lines in Figs. 5 and 6 are the least-squares fit to the T_1 data, $\log(1/T_1) = n * \log(T) - C$ where $n = 6.2$, $C = 2.1$ for CN-metHb, and $n = 6.3$, $C = 2.8$ for Im-metHb. At 40–60 K the temperature-dependent contributions to the linewidth at $g = 3.5$ were used to estimate T_2 for CN-metHb. At 105 and 120 K the temperature dependent contributions to the linewidths were used to estimate T_2 for Im-metHb. The open symbols in Figs. 5 and 6 are the values of T_1 and T_2 for Fe(III) that were used in the calculations to simulate the effect of the Fe(III) on the nitroxyl T_m and T_1 as discussed below.

The temperature dependence of the nitroxyl ESE curves was analyzed using Eqs. 4–6 with $\tau_c = \sqrt{(T_{1f}T_{2f})}$ for Fe(III). The following procedure was used for each complex. For data between 10 and 25 K the Fe(III) T_1 and T_2 values were estimated by interpolation/extrapolation of the experimental SR and ESE data shown in Figs. 5 and 6. Initially it was assumed that $J = 0$ and r was adjusted to fit the experimental data. The average of the r values from these data sets was then used for all the data, including data between 10 and 25 K, treating iron T_1 and T_2 as adjustable parameters. Values of iron T_1 above 25 K were extrapolated linearly using the least-squares fit to the data. A smooth curve was used to extrapolate $1/T_2$, intersecting the $1/T_1$ curve at ~40 K. These estimated values were then adjusted to fit the experimental data. Since the most likely source of uncertainty in the relaxation rates is uncertainty in sample temperature, T_1 and T_2 were both adjusted following the trends shown in Figs. 5 and 6. The adjusted values used in fitting the ESE data for CN-metHb-MSL and Im-metHb-ISL are shown as open symbols in Figs. 5 and 6, respectively. Although there is some scatter, it is clear that the values of T_1 and T_2 required to fit the ESE data are within experimental uncertainty of the measured values for the low-spin Fe(III) center between 6 and 25 K. The calculated decay curves are shown as dashed lines in Fig. 4. Both the shapes and the temperature dependence of the ESE decay curves are dependent on r. The values of r that were used to simulate the ESE decay curves are included in Table 1. A change in r by ~1.0 Å caused a detectable deterioration in the agreement between the experimental and calculated data. The shapes of the decay curves also depend upon J. Spin-spin interaction dominated by exchange is inconsistent with the observed decay shapes. The possibility of $J < 1$–2 G cannot be ruled out. However, addition of an exchange contribution did not improve the fit to the data.

TABLE 1 Iron-nitroxyl interspin distances for spin-labeled hemoglobins (Å)

Sample	CW range*	ESE‡	SR§
Im-metHb-ISL	14–17	15.5	15
CN-metHb-ISL	14–17	15	15
CN-metHb-MSL	14–17	15.5	15.5

*Approximate range of interspin distances for which some orientation of the interspin vector relative to the nitroxyl axes gives qualitative agreement with the CW spectra at low temperature.

‡Value of r obtained by analysis of nitroxyl T_m using Eqs. 4–6 and the temperature-dependent Fe(III) relaxation rates. Uncertainty ±1 Å.

§Value of r obtained by analysis of nitroxyl T_1 using Eqs. 1 and 2 and the temperature-dependent Fe(III) relaxation rates. Uncertainty ±1 Å.

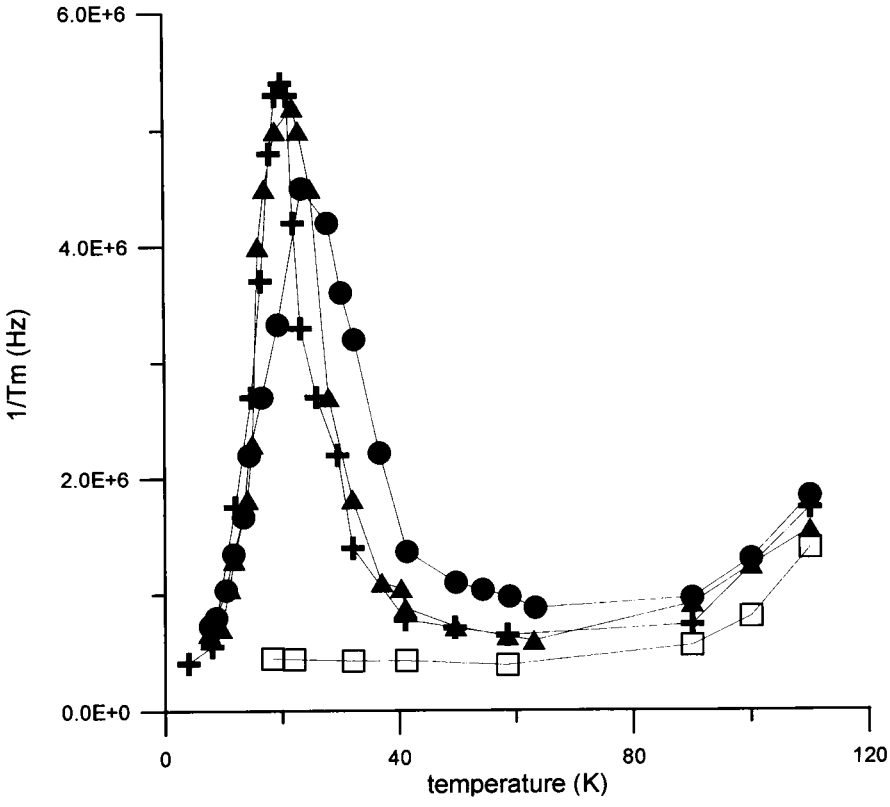

FIGURE 3 Temperature dependence of $1/T_m$ at the center of the nitroxyl signal in oxyHb-ISL (□), CN-metHb-ISL (+), CN-metHb-MSL (▲), and Im-metHb-ISL (●). Although the ESE curves were not single exponentials, a single exponential fit was used to obtain a qualitative estimate of the temperature dependence of T_m. The lines connect the data points.

SR

Interaction with the rapidly relaxing Fe(III) center decreases the nitroxyl T_1. Values of T_1 obtained by SR for two independent preparations of oxy-Hb-ISL are shown in Fig. 7. The solid line through the data for oxy-Hb-ISL in Fig. 7 is the least-squares fit to: $\log(1/T_1) = 2.24 \log(T) - 0.767$. This temperature dependence is typical of nitroxyl radicals (Nakagawa et al., 1992; Du et al., 1995). For the spin-labeled low-spin met-hemoglobins the SR data for the nitroxyl is a distribution of exponentials due to anisotropy in the low-spin Fe(III) g values and in the spin-spin coupling. The data are not accurately represented by a fit to a single exponential. However, a single-exponential fit provides a qualitative measure of the magnitude of the effect of the Fe(III) on the nitroxyl. The single exponential fits to the nitroxyl data for three spin-labeled complexes are shown in Fig. 7, which clearly shows the substantial impact of the Fe(III).

Typical SR curves for the nitroxyl signal in CN-metHb-MSL at three temperatures are shown in Fig. 8. The SR data were analyzed using Eqs. 1 and 2, following a procedure analogous to that used for the ESE data. The values of r used to simulate the curves are given in Table 1. The simulated curves are superimposed in Fig. 8. Addition of an exchange contribution did not improve the fit to the experimental data. The values of T_1 and T_2 used to simulate the SR curves for CN-metHb-MSL and Im-metHb-ISL are included in Figs. 5 and 6, respectively, and are in good agreement with the directly measured values and with the values required to match the ESE data. Since the B term in Eq. 1 and 2 dominates for these complexes, the calculated nitroxyl SR curves are more sensitive to the iron T_2 than to T_1. However, above ~40 K it appears that $T_1 \sim T_2$ (Figs. 5 and 6).

DISCUSSION

The values of r obtained by ESE and SR (Table 1) agree within experimental uncertainty and fall within the range that was estimated by qualitative computer modeling calculations and simulations of the low-temperature CW spectra. There was no evidence of an exchange interaction. The dipolar interactions at these relatively short distances are large enough relative to the anisotropy of the nitroxyl nitrogen hyperfine that orientation-selected spectroscopy is difficult in frozen solution. For longer interspin distances (and therefore smaller maximum dipolar splittings) it should be possible to examine orientation-selected relaxation data. Since the exchange interaction is isotropic and the dipolar interaction is anisotropic, orientation-selected spectra will help to distinguish the two contributions. There was no evidence of multiple conformations in SR and ESE experiments. Substantial populations of conformations with interspin distances shorter than ~12 Å can be ruled out on the basis of the absence of resolved spin-spin splitting in the CW spectra at low temperature. In addition, if larger spin-spin interaction due to shorter interspin distances were present it would be reflected in the temperature dependence of nitroxyl T_m. Substantial populations with significantly longer interspin distances would have resulted in a slowly relaxing component in the SR or ESE data. Components with similar interspin distances would be difficult to distinguish without

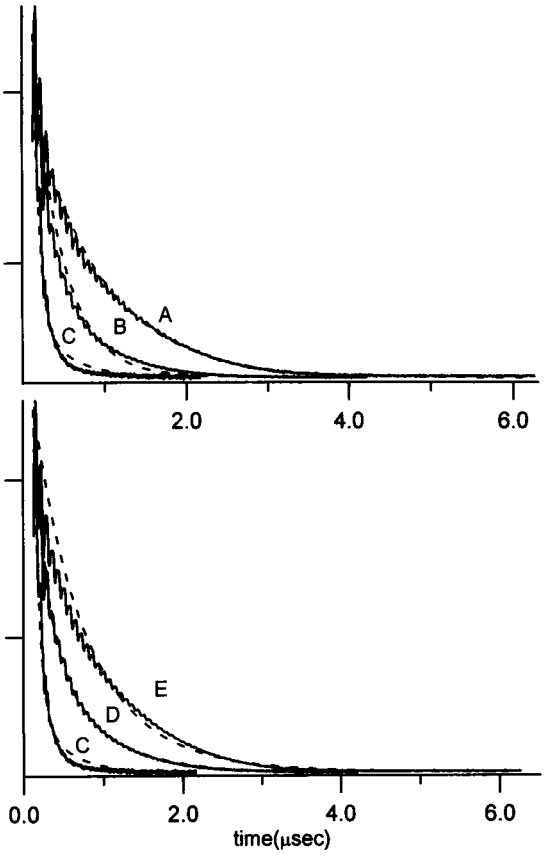

FIGURE 4 Temperature dependence of ESE decays at the center of the nitroxyl signal for CN-metHb-MSL in 1:1 buffer glycerol at 9.19 GHz. (*A*) 8 K, (*B*) 12 K, (*C*) 23 K, (*D*) 37 K, and (*E*) 59 K. The data at 23 K are shown in both halves of the figure. The dashed lines were calculated using Eqs. 3–6 with r = 15.5 Å, J = 0, and $\tau_c = \sqrt{(T_{1f}T_{2f})}$ for Fe(III). See discussion in text for additional parameters.

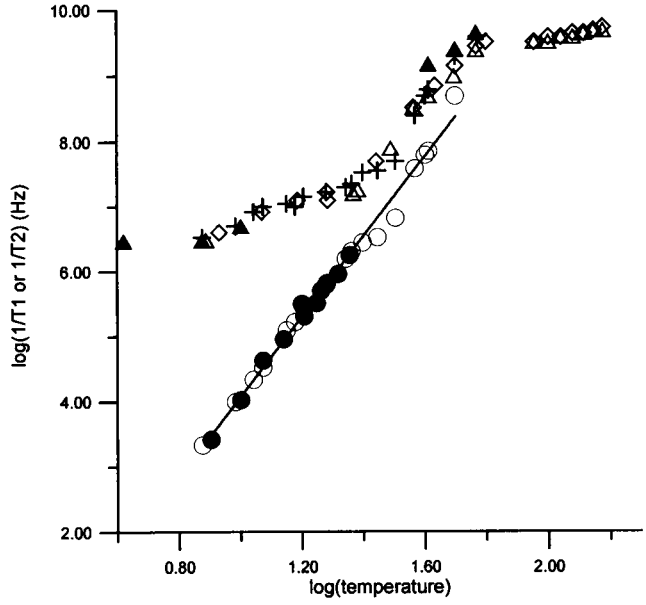

FIGURE 5 Temperature dependence of electron spin relaxation rates for low-spin Fe(III) in CN-metHb: (●) T_1 measured by SR, and (▲) T_2 measured by ESE between 7 and 10 K and by temperature-dependent contribution to linewidth at 40, 50, and 60 K. The solid line is the least-squares fit to the T_1 data: $\log(1/T_1) = 6.2 * \log(T) - 2.1$. The open symbols are values obtained by analysis of the effect of the low-spin Fe(III) on relaxation rates for the spin label in CN-metHb-MSL: (○) T_1 and (+) T_2 used in Eqs. 4–6 with r = 15.5 Å and $\tau_c = \sqrt{(T_{1f}T_{2f})}$ to analyze nitroxyl T_m; (◇) T_2 used in Eqs. 1 and 2 with r = 15.5 Å to analyze nitroxyl T_1, and for CN-metHb-ISL (△) T_2 used in Eqs. 1 and 2 with r = 15 Å to analyze nitroxyl T_1.

orientation-selected data. The combined data suggest that the observed conformation is the one denoted as B by McConnell and Hamilton (1968) and McConnell et al. (1969), in which the EPR and molecular modeling both suggest a distance of ~15 Å.

Manoharan, Rifkind and co-workers (Antholine et al., 1985; Manoharan et al., 1990) studied interaction between a nitroxyl spin label at position β93 and Cu(II) at several locations in human and horse hemoglobin. In human hemoglobin Cu(II) at the "high affinity" site near the amino terminal residue of the β chain was concluded to be 17 Å from the nitroxyl at 77 K but 7 Å at 293 K, based on the Leigh (1970) model. In that report the temperature dependence of the metal T_1 does not appear to have been taken into account. In horse hemoglobin, which lacks this high affinity site, Cu(II) was stated to bind 10–13 Å from the nitroxyl (Antholine et al., 1985). When Cu(II) and Ni(II) replaced iron in the heme group, the metal-nitroxyl distance was estimated as 7.4–9.9 Å for various labels (Manoharan et al., 1990). However, as we have discussed previously, the Leigh model should not be applied when the metal relaxation times are as long as for Cu(II)porphyrins at liquid nitrogen temperatures (Eaton and Eaton, 1988b). The effect of Cu(II) on the nitroxyl relaxation was observed in CW microwave power saturation experiments, but this effect was stated not to be the cause of the changes in the nitroxyl EPR spectrum (Antholine et al., 1985). Time-domain EPR studies of spin-labeled Cu(II) hemoglobin will be reported separately.

Between 8 and 20 K the temperature dependence of $1/T_1$ for the low-spin Fe(III) fit to $\log(1/T_1) = n \log(T) + C$ with n = 6.2 and C = –2.1 for CN-MetHb and n = 6.3, C = –2.8 for ImMetHb (Figs. 5 and 6). Allen et al. (1982) examined the temperature dependence of T_1 for low-spin Fe(III) proteins. Between ~5 and 15 K a fit of the data to $\log(1/T_1) = n \log(T)$ gave n = 6.22 to 6.34 for four heme proteins and n = 5.67 for ferredoxin. The values of n were interpreted in terms of the fractal dimensions of the protein (Allen et al., 1982). More recently Drews et al. (1990) concluded, based on studies of copper as well as iron, that "the chain fractal dimension is not simply correlated with relaxation behavior in proteins." For bis(*N*-methylimidazole) (iron tetraphenylporphyrin)$^+$ a value of n = 7.0 was found (Rakowsky et al., 1995). The similarity in n for the small-molecule low-spin Fe(III) porphyrin and the low-spin Fe(III) in heme proteins suggests that n is determined more by the local heme environment than by the long-range structure of the protein.

The analysis of the nitroxyl SR curves provides estimates of the iron relaxation rates at higher temperatures than are accessible by direct measurements. Values of the Fe(III) $T_1 \sim T_2$ required to fit the impact of the Fe(III) on the nitroxyl

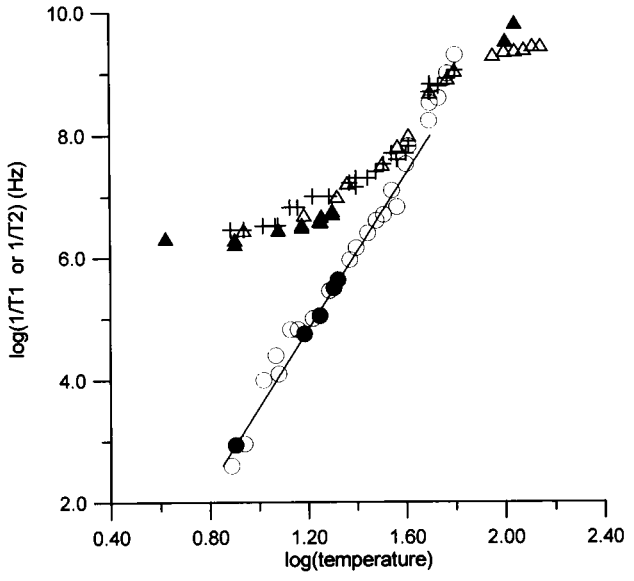

FIGURE 6 Temperature dependence of electron spin relaxation rates for low-spin Fe(III) in Im-metHb: (●) T_1 measured by SR, and (▲) T_2 measured by ESE between 4 and 20 K and by temperature- dependent contribution to linewidth at 105 and 120 K. The solid line is the least-squares fit to the T_1 data: $\log(1/T_1) = 6.3 * \log(T) - 2.8$. The open symbols are values obtained by analysis of the effect of the low-spin Fe(III) on relaxation rates for the spin label in Im-metHb-ISL: (○) T_1 and (+) T_2 used in Eqs. 4–6 with r = 15.5 Å and $\tau_c = \sqrt{(T_{1f}T_{2f})}$ to analyze nitroxyl T_m; (△) T_2 used in Eqs. 1 and 2 with r = 15 Å to analyze nitroxyl T_1.

T_m and T_1 at 40–60 K for CN-metHb-ISL and CN-metHb-MSL are consistent with estimates based on the temperature-dependent contribution to the CW lineshape of CN-metHb.

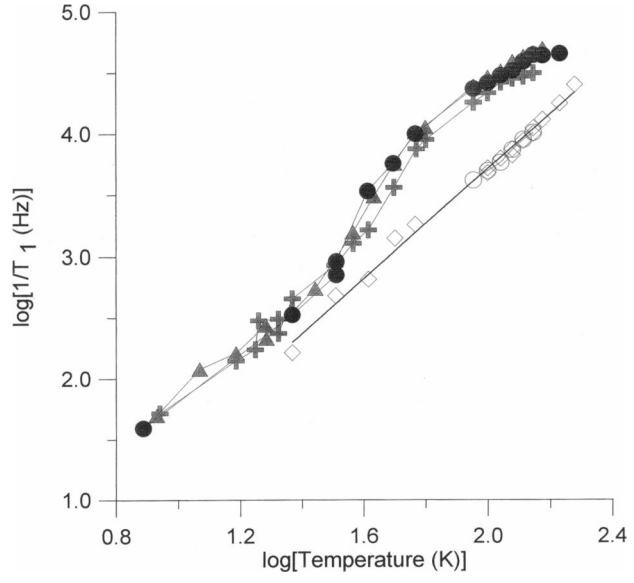

FIGURE 7 Temperature dependence of nitroxyl T_1 measured at the center of the spectrum in 1:1 buffer:glycerol solution in the absence and presence of low-spin Fe(III) at 9.2 GHz: (◇, ○), oxyHb-ISL, two independent preparations; (▲), CN-metHb-MSL; (●), CN-metHb-ISL; (+), Im-metHb-ISL. The solid line through the data for oxy-Hb-ISL is the least-squares fit to $\log(1/T_1) = 2.24 \log(T) - 0.767$. The other lines connect the data points.

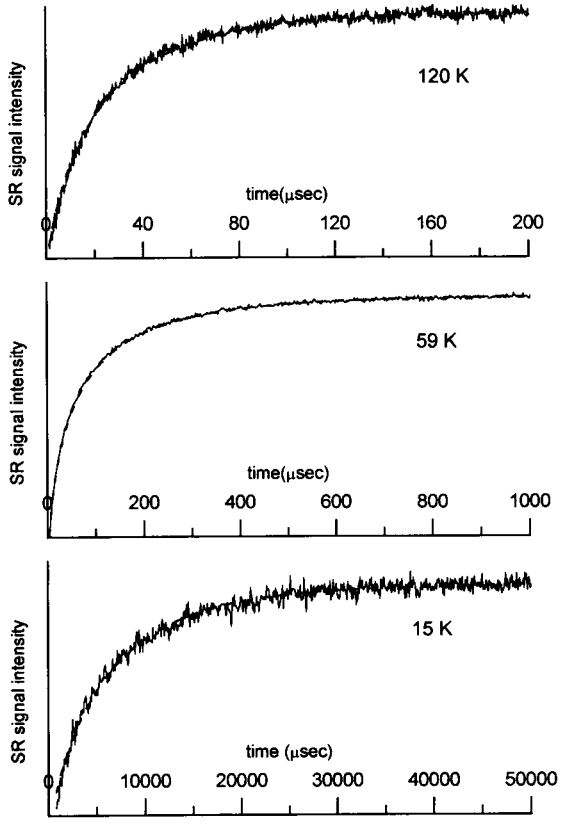

FIGURE 8 SR curves for the nitroxyl signal in CN-metHb-MSL in 1:1 buffer:glycerol at 9.2 GHz and 15, 59, and 120 K. The dashed lines were calculated with Eqs. 1 and 2, and r = 15.5 Å. See text for other parameters.

For Im-metHb-ISL the iron relaxation rates required to fit the effect of the Fe(III) on nitroxyl T_1 at 100–120 K are consistent with estimates based on the temperature dependent contribution to the CW linewidth for Im-MetHb. Above ~80 K the iron relaxation rates are less strongly temperature dependent than at lower temperatures. This behavior was observed for the three spin-labeled hemoglobin samples that were examined. The slower change in relaxation rate at higher temperature (Figs. 5 and 6) is consistent with approach to the high-temperature limit of a Raman process.

The maximum interspin distance for which significant effect of a fast relaxing center on T_1 for a slowly relaxing partner can be observed depends upon $T_{1s}°$, S for the fast relaxing center, and the relaxation rates for the fast relaxing center (Eq. 1). For low-spin Fe(III) (S = ½) with relaxation rates comparable to those observed for the methemoglobins interacting with a radical with $T_{1s}°$ similar to that for a nitroxyl, detectable effects are predicted for distances up to ~20 Å. For metals with larger S and/or faster relaxation rates, observable effects are expected for interspin distances as long as ~35 Å. Observation of effects on T_m for the slowly relaxing center that result from collapse of spin-spin splitting to a faster relaxing center as described by Eqs. 4–6 requires a spin-spin splitting in Hz that is greater than the spin packet linewidth, $1/T_2$. For typical organic radical relaxation times at low temperature this should be observable for distances as

long as ~25 Å. To define the full kinetic range from slow to fast metal relaxation relative to the spin-spin interaction requires observation over a temperature range that encompasses $\tau_c = \sqrt{(T_{1f}T_{2f})} \gg$ spin-spin splitting to $\tau_c = \sqrt{(T_{1f}T_{2f})} \ll$ spin-spin splitting. Metal ions for which this range of relaxation times is likely to be observable between 4 and 70 K include, e.g., low-spin and high-spin Fe(III), high-spin Co(II), and $S = \frac{1}{2}$ iron-sulfur clusters.

CONCLUSIONS

Values of T_1 and T_2 for low-spin Fe(III) measured by SR and ESE permit quantitative interpretation of the impact of the rapidly relaxing iron center on the SR and ESE curves for a nitroxyl radical to which it is spin coupled. The two techniques provide consistent values for the interspin distance. Analysis of the nitroxyl SR and ESE data at temperatures where the iron relaxation rates are too fast to measure directly provide information on the Fe(III) relaxation rates. These complexes demonstrate the utility of ESE and SR measurements of the signal for the slower-relaxing partner to determine interspin distance and to probe the relaxation behavior of the faster relaxing partner.

The financial support of this work by National Institutes of Health grant GM 21156 and a National Science Foundation shared instrumentation grant (CHE-9318714) for purchase of the Bruker ESP 380E are gratefully acknowledged. Professor Winslow Caughey and Dr. Vijaya Sampath, Colorado State University, graciously guided our first isolation of hemoglobin and shared with us their enthusiasm for this fascinating protein.

REFERENCES

Allen, J. P., J. T. Colvin, D. G. Stinson, C. P. Flynn, and H. J. Stapleton. 1982. Protein conformation from electron spin relaxation data. *Biophys. J* 38:299–310.

Antholine, W. E., F. Taketa, J. T. Wang, P. T. Manoharan, and J. M. Rifkind. 1985. Interaction between bound cupric ion and spin-labeled cysteine β-93 in human and horse hemoglobins. *J. Inorg. Biochem.* 25:95–108.

Antonini, E., and M. Brunori. 1971. Hemoglobin and Myoglobin in their Reactions with Ligands. North-Holland Publishing Co., Amsterdam. 19.

Asakura, T., and H. R. Drott. 1971. Evidence of heme-heme interaction in heme-spin-labeled hemoglobin. *Biochem. Biophys. Res. Commun.* 44: 1199–1204.

Asakura, T., and P.-W. Lau. 1978. Sequence of oxygen binding by hemoglobin. *Proc. Natl. Acad. Sci. USA.* 75:5462–5465.

Asakura, T., M. Tamura, and M. Shin. 1972. Enzymatic reduction of spin-labeled ferrihemoglobin. *J. Biol. Chem.* 247:3693–3701.

Berstain, F. C., T. F. Koetzle, G. J. B. Williams, E. F. Meyer Jr., M. D. Brice, J. R. Rodgers, O. Kennard, T. Shimanouchi, and M. Tasumi. 1977. The Protein Data Bank: a computer-based archival file for macromolecular structures. *J. Mol. Biol.* 112:535–542.

Bloembergen, N. 1949. On the interaction of nuclear spins in a crystalline lattice. *Physica.* 15:386–426.

Bloembergen, N., E. M. Purcell, and R. V. Pound. 1948. Relaxation effects in nuclear magnetic resonance absorption. *Phys. Rev.* 73:679–712.

Bloembergen, N., S. Shapiro, P. S. Pershan, J. O. Artman. 1959. Cross-relaxation in spin systems. *Phys. Rev.* 114:445–459.

Brocklehurst, K., and G. Little. 1973. Reactions of papain and of low-molecular weight thiols with some aromatic disulphides. *Biochem. J.* 133:67–80.

Caughey, W. S., and J. A. Watkins. 1985. Autooxidation of hemoglobin. *In* CRC Handbook of Methods for Oxy Radical Research. R. A. Greenwald, editor. CRC Press, Boca Raton, FL. 95–104.

Chien, J. C. W. 1979. Electron paramagnetic resonance crystallography of spin-labeled hemoglobin-protein fine structures. *J. Mol. Biol.* 133: 385–398.

Chien, C. W., C. Dickinson, F. W. Snyder Jr., and K. H. Mayo. 1980. Circular dichroism and spin-label studies of carp hemoglobin. *J. Mol. Biol.* 142:75–91.

Dilorio, E. E. 1981. Preparation of derivatives of ferrous and ferric hemoglobin. *Methods Enzymol.* 76:57–72.

Drago, R. S. 1992. Physical Methods for Chemists, 2nd ed. Saunders College Publishing, Fort Worth. 290–295.

Drews, A. R., B. D. Thayer, H. J. Stapleton, G. C. Wagner, G. Giuliarelli, and S. Cannistraro. 1990. Electron spin relaxation measurements on the blue-copper protein plastocyanin: deviations from a power law temperature dependence. *Biophys. J.* 57:157–162.

Du, J.-L., G. R. Eaton, and S. S. Eaton. 1994. Effect of molecular motion on electron spin phase memory times for copper(II) complexes in doped solids. *Appl. Magn. Reson.* 6:373–378.

Du, J.-L., G. R. Eaton, and S. S. Eaton. 1995. Temperature, orientation, and solvent dependence of electron spin lattice relaxation rates for nitroxyl radicals in glassy solvents and doped solids. *J. Magn. Reson.* In press.

Du, J.-L., K. M. More, S. S. Eaton, and G. R. Eaton. 1992. Orientation dependence of electron spin phase memory relaxation times in copper(II) and vanadyl complexes in frozen solution. *Isr. J. Chem.* 32:351–355.

Dzuba, S. A., K. M. Salikhov, and Y. D. Tsvetkov. 1981. Slow rotations of methyl groups in radicals studied by pulse ESR spectroscopy. *Chem. Phys. Lett.* 79:568–572.

Eaton, S. S., and G. R Eaton. 1977. Electron paramagnetic resonance sample cell for lossy samples. *Anal. Chem.* 49:1277–1278.

Eaton, G. R., and S. S. Eaton. 1988a. EPR studies of long-range intramolecular electron-electron exchange interaction. *Acct. Chem. Res.* 21:107–113.

Eaton, S. S., and G. R. Eaton. 1988b. Interaction of spin labels with transition metal ions, Part 2. *Coord. Chem. Rev.* 83:29–72.

Eaton, G. R., and S. S. Eaton. 1989. Resolved electron-electron spin-spin splittings in EPR spectra. *Biol. Magn. Reson.* 8:339–397.

Eaton, S. S., K. M. More, B. M. Sawant, P. M. Boymel, and G. R. Eaton. 1983. Metal-nitroxyl interactions. 29. EPR studies of spin-labeled copper complexes in frozen solution. *J. Magn. Reson.* 52:435–449.

Grassetti, D. R., and J. F. Murray Jr. 1967. Determination of sulfhydryl groups with 2,2′- or 4,4′-dithiopyridine. *Arch. Biochem. Biophys.* 119: 41–49.

Hartmann, D., R. Philipp, K. Schmadel, J. J. Birktoft, L. J. Banszak, and W. E. Trommer. 1991. Spatial Arrangement of coenzyme and substrates bound to L-3-hydroxyacyl-CoA dehydrogenase as studied by spin-labeled analogues of NAD^+ and CoA. *Biochemistry.* 30:2782–2790.

Ho, C., J. J. Baldessare, and S. Charache. 1970. Electron paramagnetic resonance studies of spin-labeled hemoglobins and their implications to the nature of cooperative oxygen binding to hemoglobin. *Proc. Natl. Acad. Sci. USA.* 66:722–729.

Kelleher, M. J. 1993. The azido human methemoglobin controversy: is there evidence for a quaternary structure-spin state linkage or not? *Acct. Chem. Res.* 26:154–159.

Kispert, L. D., M. K. Bowman, J. R. Norris, and M. S. Brown. 1982. Electron spin echo studies of the internal motion of radicals in crystals: phase memory vs. correlation time. *J. Chem. Phys.* 76:26–30.

Kulikov, A. V., and G. I. Likhtenshtein. 1977. The use of spin relaxation phenomena in the investigation of the structure of model and biological systems by the method of spin labels. *Adv. Mol. Relax. Interact. Processes.* 10:47–69.

Leigh, J. S. 1970. ESR rigid-lattice line shape in a system of two interacting spins. *J. Chem. Phys.* 52:2608–2612.

Manoharan, P. T., J. T. Wang, K. Alston, and J. M. Rifkind. 1990. Spin label probes of the environment of cysteine β-93 in hemoglobin. *Hemoglobin.* 14:41–67.

Marden, M. C., L. Kiger, J. Kister, B. Bohn, and C. Poyart. 1991. Coupling of ferric iron spin and allosteric equilibrium in hemoglobin. *Biophys. J.* 60:770–776.

McConnell, H. M. 1971. Spin-label studies of cooperative oxygen binding to hemoglobin. *Annu. Rev. Biochem.* 40:227–236.

McConnell, H. M., and J. C. A. Boeyens. 1967. Spin-label determination of enzyme symmetry. *J. Phys. Chem.* 71:12–14.

McConnell, H. M., W. Deal, and R. T Ogata. 1969. Spin-labeled hemoglobin derivatives in solution, polycrystalline suspensions, and single crystals. *Biochemistry.* 8:2580–2585.

McConnell, H. M., and C. L. Hamilton. 1968. Spin-labeled hemoglobin derivatives in solution and in single crystals. *Proc. Natl. Acad. Sci. USA.* 60:776–781.

Moffat, J. K. 1971. Spin-labeled hemoglobins: a structural interpretation of electron paramagnetic resonance spectra based on x-ray analysis. *J. Mol. Biol.* 55:135–146.

Nakagawa, K., M. B. Candelaria, W. W. C. Chik, S. S. Eaton, and G. R. Eaton. 1992. Electron-spin relaxation times of chromium(V). *J. Magn. Reson.* 98:81–91.

Ogata, T., and H. M. McConnell. 1971. The binding of a spin-labeled triphosphate to hemoglobin. *Cold Spring Harbor Symp.* 36:325–336.

Quine, R. W., G. R. Eaton, and S. S. Eaton. 1987. Pulsed EPR spectrometer. *Rev. Sci. Instrum.* 58:1709–1723.

Quine, R. W., S. S. Eaton, and G. R. Eaton. 1992. Saturation recovery electron paramagnetic resonance spectrometer. *Rev. Sci. Instrum.* 63: 4251–4262.

Rakowsky, M. H., K. M. More, A. V. Kulikov, G. R. Eaton, and S. S. Eaton. 1995. Time-domain electron paramagnetic resonance as a probe of electron-electron spin-spin interaction in spin-labeled low-spin iron porphyrins. *J. Amer. Chem. Soc.* 117:2049–2057.

Salikhov, K. M., and Y. D. Tsvetkov. 1979. Electron spin-echo studies of spin-spin interactions in solids. *In* Time Domain Electron Spin Resonance. L. Kevan and R. N. Schwartz, editors. Wiley, New York.

Scheler, W., G. Schoffa, and F. Jung. 1957. Light absorption and paramagnetic susceptibility. *Biochem. Z.* 329:232–246.

Scholes, C. P., A. Lapidot, R. Mascarenhas, T. Inubushi, R. A. Isaacson, and G. Feher. 1982. Electron nuclear double resonance (ENDOR) from heme and histidine nitrogens in single crystals of aquometmyglobin. *J. Am. Chem. Soc.* 104:2724–2735.

Shaanan, B. 1983. Structure of oxyhaemoglobin at 2.1 Å resolution. *J. Mol. Biol.* 171:31–59.

Steinhoff, J. 1990. Residual motion of hemoglobin-bound spin labels and protein dynamics: viscosity dependence of the rotational correlation times. *Eur. Biophys. J.* 18:57–62.

Toy, A. D., S. H. H. Chaston, J. R. Pilbrow, and T. D. Smith. 1971. An electron spin resonance study of the copper(II) chelates of certain monothio-β-diketones and diethyldithiocarbamate. *Inorg. Chem.* 10: 2219–2225.

Tsvetkov, Y. D., and S. A. Dzuba. 1990. Pulsed ESR and molecular motions. *Appl. Magn. Reson.* 1:179–194.

Wolf, E. L. 1966. Diffusion effects in the inhomogeneously broadened case: high-temperature saturation of the F-center electron spin resonance. *Phys. Rev.* 142:555–569.

Zhidomirov, G. M., and K. M. Salikhov. 1969. Contribution to the theory of spectral diffusion in magnetically diluted solids. *Sov. Phys. JETP.* 29:1037–1040.